We are IntechOpen,
the world's leading publisher of
Open Access books
Built by scientists, for scientists

4,800
Open access books available

122,000
International authors and editors

135M
Downloads

Our authors are among the

154
Countries delivered to

TOP 1%
most cited scientists

12.2%
Contributors from top 500 universities

CLARIVATE ANALYTICS
BOOK CITATION INDEX
INDEXED

WEB OF SCIENCE™

Selection of our books indexed in the Book Citation Index
in Web of Science™ Core Collection (BKCI)

Interested in publishing with us?
Contact book.department@intechopen.com

Numbers displayed above are based on latest data collected.
For more information visit www.intechopen.com

Digital Signal Processing for Acoustic Emission

Paulo R. Aguiar, Cesar H.R. Martins, Marcelo Marchi and Eduardo C. Bianchi

Additional information is available at the end of the chapter

1. Introduction

Fast advances in several signal processing techniques, along with cost-effective digital technologies for their implementation, are ready to address important manufacturing and machine monitoring issues for which no solution currently exists. Among new technologies are advances in wavelet and time-frequency signal analysis. By virtue of their ability to characterize both transient phenomena and persistent harmonic structure, they appear well-matched to the signals associated with rotating machinery. Other recent developments, such as higher-order spectral theory, could also possibly contribute in these applications.

Because of the complexity into detection and categorization of faults are normally difficult to solve analytically or through mathematical modelling, and usually require human intelligence, thus, higher-level techniques such as neural networks and statistical pattern recognition and classification have demonstrated improvements over traditional approaches. These methods, with appropriately directed research, may offer solutions for the critical technology needs in manufacturing and machine monitoring. The growing interest in the use of artificial intelligence for the solution of engineering problems is visible from the considerable number of articles published in the last decade [1].

Thus, the present chapter aims to present results of statistical tools to detect faults in machining processes, by digitally processing the acoustic emission signals generated during the process.

2. Monitoring and process control of machining processes

The implementation of intelligent processes in industries utilizing computer numerically controlled machining is increasing rapidly. However, these systems are not enough reliable to operate without human interference so far. It is common to observe operators of CNC machines correct the process parameters or identify the end of the tool life [2].

INTECH
open science | open minds

In the grinding process, the workpiece quality depends to a great extent on the experience of the operator. This occurs because grinding is a very complex process affected by so many factors that a reproducible result is rarely obtained. The most important one is that the cutting ability of the grinding wheel changes considerably during the grinding time. In practice the grinding process is carried out with cutting parameters that are safe but not optimal. Another and no less important parameter to be controlled in grinding is dressing, which is the process of conditioning the grinding wheel surface in order to reshape the wheel when it has lost its original shape through wear [3-4].

Thus, there are three main goals related to grinding process monitoring: detection of problems during machining; provision of information necessary to optimize the process; and the contribution to the development of a database needed to determine the control parameters [5].

The use of acoustic emission (AE) to monitor and control the grinding process is a relatively recent technology [6], besides being more sensitive to the grinding condition variations, when compared with the force and power measurements [7], standing as a promising technique to the process monitoring.

Acoustic emission is the phenomenon in which elastic or stress waves are emitted from a rapid, localized change of strain energy in a material. Typically frequencies are in the range of 100 kHz to 2 MHz, well above the vibration frequencies of most machines and surroundings. At grinding process the AE signals are directly generated in the deformation zone. Thus, an important assumption is made: AE generated during the grinding process is assumed to contain information related to the micro mechanical phenomena of the grinding process and thus conditions of its components [8].

With the objective to determine features of the machining processes from the AE signal, techniques of signal processing are applied, and may include: root mean square (RMS), constant false alarm rate (CFAR), mean value dispersion statistic (MVD) etc. Features of the machining processes may be extracted as part of the particular monitoring system [9-10].

2.1. Root mean square (RMS)

The root mean square of the raw AE signal can be expressed by Equation (1):

$$AE_{RMS} = \sqrt{\frac{1}{\Delta T} \int_0^{\Delta t} AE^2(t) dt} = \sqrt{\frac{1}{N} \sum_{i=1}^{N} AE^2(i)} \tag{1}$$

Where ΔT is the integration time constant and N is the number of discrete AE data within ΔT. AE_{RMS} can be obtained by using an analog RMS filter or digitally by calculating with a chosen ΔT according to the right part of the equation. There is no general rule in selecting suitable ΔT to obtain AE_{RMS}, however ΔT=1 ms provides a good resolution for grinding process, and have been used for many researchers.

2.2. Constant false alarm rate (CFAR)

Constant false alarm rate (CFAR) is a statistic tool employed in detection of events, which is described by [11]:

$$T_{pl}\left(X\right)=\sum_{k=0}^{M-1} X_k^{\upsilon} \tag{2}$$

Where the X_k is the kth magnitude-squared FFT bin, υ is a changeable exponent and 2M is the total FFT bins. Respectively υ=1 and υ=∞ correspond to the energy detector and max{X_k}. Although υ between 2 and 3 provides a good performance for a wide frequency band of the studied signal, this statistic needs pre-normalized data. Due to the fluctuation of the AE signal during the grinding process, a constant false alarm rate (CFAR) power-law [12] is used. The CFAR power-law is based on an assumption that the spectrum of AE signal is flat. An alternative version of this tool was employed due to system distortions, which is expressed by the following equation [13].

$$T_{bcpl}\left(X\right)=\frac{\displaystyle\sum_{k=n1}^{n2} X_k^{\upsilon}}{\left(\displaystyle\sum_{n1}^{n2} X_k\right)^{\upsilon}} \tag{3}$$

Where T_{bcpl} is clearly not affected by signal amplitude. This version of the CFAR power-law statistics is band-limited by $n1$ and $n2$.

2.3. Mean value dispersion statistic (MVD)

The mean-value deviance (MVD) statistic quantifies in a certain way the average deviation of observations from its mean value. Unusually large value of $T_{mvd}(X)$ implies such deviation is too great to be explained using a simple exponential distribution model. This statistic is sensitive to small outliers, that is, observations with extremely small values [14].

The MVD statistic was used successfully in burn detection [15], and is defined by Equation (4).

$$T_{mvd}\left(X\right)=\frac{1}{M}\sum_{k=0}^{M-1}\log\left[\frac{\bar{X}}{X_k}\right] \tag{4}$$

Where $\bar{X}$ is the mean value of $\{X_k\}$; $2M$ is the total number of FFT bins, and is the kth magnitude-squared FFT bin.

2.4. Kurtosis and skewness statistics

The measurement if the distribution tail is longer than other is made by skew. In case of kurtosis, the tail size is expressed. Both statistics are utilized as an indicator to the acoustic

emission variations. Thus, abrupt changes in the AE signal may result in spikes in these statistics. The Equation (5) shows the way of calculating kurtosis of an x signal.

$$K = \sum \frac{(x-\mu)^4}{N\sigma^4} - 3 \tag{5}$$

Where μ is the mean of x, N the number of samples in the range considered and σ the standard deviation.

Similarly, the expression given in Equation (6) is used to calculate skewness.

$$S = \sum \frac{(x-\mu)^3}{N\sigma^3} \tag{6}$$

2.5. Ratio of power (ROP)

It is instinctive to think about the different behaviours expected for a good part or bad one by observing the frequency spectrum of the AE signal. Hence, for each block of AE data ROP is given by Equation (7).

$$ROP = \sum_{k=n_1}^{n_2} \frac{|X_k|^2}{\sum_{k=0}^{N-1} |X_k|^2} \tag{7}$$

The denumerator eliminates the local effect of power in equation, where N is the size of a block of AE data; n_1 and n_2 define a frequency range to analyse.

2.6. Autocorrelation

The time correlation of a function Φ_{xy} is defined by Oppenheim [16] in Equation (8).

$$\phi_{xy}(t) = \int_{-\infty}^{+\infty} x(t+\tau) y(\tau) d\tau \tag{8}$$

Where Φ_{xx} is commonly referred to autocorrelation of x signal.

2.7. DPO

The combination of the RMS AE signal and the cutting power signal provided a parameter to indicate burning of the workpiece in surface grinding, which has been dubbed DPO, and consists of the relation between the standard deviation of the RMS AE signal and the maximum cutting force per grinding wheel pass [17]. Equation (5) represents the DPO parameter.

$$DPO = std(AE)\max(pw) \tag{9}$$

Where *std(AE)* is the standard deviation of the RMS AE and *max(pw)* is the maximum value of cutting power in the pass.

2.8. DPKS

The DPKS statistic was developed by Dotto [18] in order to increase the sensitivity of the DPO parameter. This parameter allows to identify the exact moment when grinding burn begins, and in the case of dressing, the exact moment to stop the process. The DPKS is calculated by multiplying the standard deviation of AE by the sum of the cutting power subtracted from its standard deviation elevated to the fourth power. Equation (6) represents the calculated DPKS statistic:

$$DPKS = \left(\sum_{i=1}^{m} \left(pw(i) - std(pw) \right)^4 \right) std(AE) \tag{10}$$

Where i is the power index which varies from 1 up to m points in each pass, *pw(i)* and *std(pw)* are, respectively, the instant value of the cutting power and standard deviation of the cutting power in the pass, and *std(AE)* is the standard deviation of the RMS AE in the pass.

2.9. Artificial neural network (ANN)

According to Kwak & Song [19], neural networks are composed of many non-linear computational elements operating in parallel. Because of their massive nature and their adaptive nature in using the learning process, neural networks can perform computations at a higher rate and adapt to changes in data learning the characteristics of input signals. The usefulness of an artificial neural network comes from the ability to respond to an input pattern in a desirable fashion, after the learning phase.

The artificial neural network efficiency has proved in previous investigations in the prediction of faults at machining processes. Thus, this technique is very promising and can also be applied successfully to industrial automation in a flexible and integrated fashion.

2.9.1. Multi layer perceptron (MLP)

Nathan et al. [20] state that there are three structural layers in a network, namely the input layer (which receives input from the outside world), the hidden layer (between the input and the output layers) and the output layer (the response given to the outside world). The neurons of different layers are interconnected through weights. Thus, processing elements at different layers, interconnections between them, and the learning rules that define the way in which inputs are mapped on to the outputs constitutes a neural network. The usefulness of an ANN comes from its ability to respond to an input pattern in a desirable

fashion, after the learning phase. As such, the processing units receive inputs and perform a weighted sum of its input values using the connection weights given initially by user. This weighted sum is termed the activation value of the neuron, given by:

$$u = \sum w_i x_i + \theta \tag{11}$$

where w_{ij} is the weight interconnecting two nodes i and j; x_i is the input variable; and u is the threshold value. During the forward pass through the network, each neuron evaluates an equation that expresses the output as a function of the inputs. Using the right kind of transfer function is therefore essential. A sigmoidal function can be used for this purpose, and is given by:

$$f(x) = \frac{1}{\left(1 + e^{-u}\right)} \tag{12}$$

Depending on the mismatch of the predicted output with the desired output, the weights are adjusted by back-propagation of error, so that the current mean square error (MSE) given by the following equation is reduced:

$$MSE = \frac{1}{2NK} \sum_{n=1}^{N} \sum_{k=1}^{K} \left(b_{nk} - S_{nk}\right)^2 \tag{13}$$

where N is the number of patterns in the training data, K is the number of nodes in the network, b_{nk} is the target output for the nth pattern and s_{nk} is the actual output for the nth pattern.

Still, according to Hykin apud Nathan et al. [20], it should be noted that the MSE itself is a function of the weights, as the computation of the output uses them. During this learnig phase of the network the weights and the threshold values are adapted in order to develop the knowledge stored in the network. The weights are adjusted so as to obtain the desired output. The problem of finding the best set of weights in order to minimize the discrepancy between the desired and the actual response of the network is considered as a non-linear optimization problem. The most popularly used learning algorithm, namely the back-propagation algorithm, uses an interactive gradient-descent heuristic approach to solve this problem. Once the learning process is completed, the final set of weight values is stored, this constituting the long term memory of the network, which is used later during the prediction process.

2.9.2. The radial basis neural network

According to Musavi et al. [21] Radial Basis Function (RBF) technique provides an alternative tool to learning in neural networks. The main idea is to design a network with good generalization ability and a minimum number of nodes to avoid unnecessarily lengthy calculations as opposed to multilayer perceptron networks. The RBF classifiers which belong to the group of kernel classifiers utilize overlapping localized regions formed by simple kernel functions to create complex decision regions.

The structure of the radial basis ANN is like a MLP with three layers, an input layer, the radial basis function layer, and one linear layer output neuron [22]. This structure is shown in Figure (1).
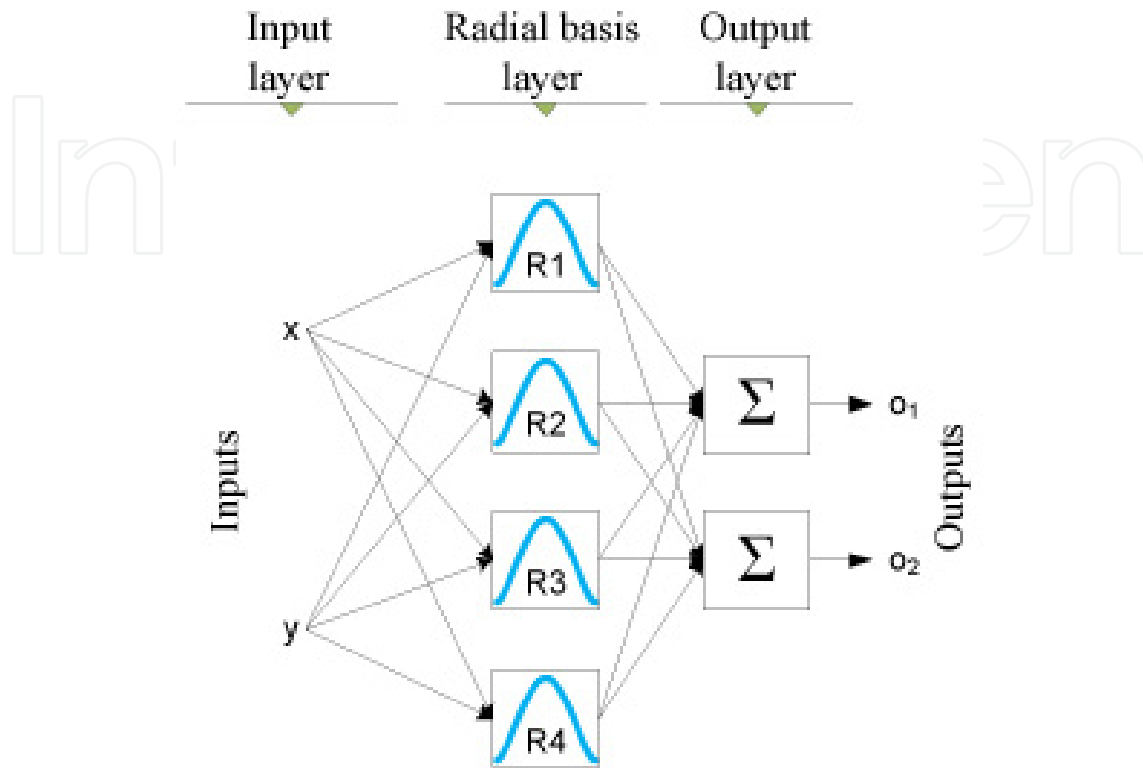

Figure 1. A generic radial basis network. Adapted from Jang [23].

The radial basis function (RBFs), which have been widely advocated [21], are approximations of the form

$$yr = \alpha + \sum_j \beta_j G\left(\left\|x - x_j\right\| / \sigma_j\right) \qquad (14)$$

for centers x_j, where $G(r) = exp(-r2/2)$, σ is the covariance matrix. Using RBFs as the basis functions, one output can be represented by

$$y = b2 + \sum_{j=1}^{n_j} w2_j \exp\left(-b1_j^2 \sum_{i=1}^{n_i} \left(w1_{ji} - x_i\right)^2\right) \qquad (15)$$

where x is the input vector with size n_i, n_i and n_j are separately the numbers of neurons used in input and the radial basis layer, $w1$ and $b1$ are the weight matrix and the bias vector with dimension n_j for the radial basis layer, $w2$ and $b2$ are the corresponding weight matrix and bias scale for the linear layer.

Just as any statistical analysis, an implied requirement for developing robust neural network models is that the training sets cover as many of the possible variations in the input and output vector as possible.

2.9.3. Adaptive neuro-fuzzy inference system (ANFIS)

The ANFIS system is based on the functional equivalence, under certain constraints, of RBF networks and Takagi-Sugeno-Kang (TSK) fuzzy systems [24-25]. A single existing output is calculated directly by weighting the inputs according to fuzzy rules, which are the knowledge base determined by a computational algorithm based on neural networks.

To produce an ANFIS model that performs well requires taking into account the initial number of parameters and the number of inputs and rules of the system [26]. These parameters are determined empirically and an initial model with equally spaced membership functions is usually created. However, this method is not always efficient because it does not show how many relevant input groups there are.

The subtractive clustering algorithm [27-28] is used to identify data distribution centers, which contain the membership curves with membership values equal to 1. The algorithm uses the cluster number or the size of the neighborhood radius and the number of iteration times. In each pass through the algorithm, the latter looks for a point that minimizes the sum of the potential with the neighboring points.

According to Lee et al. [29], ANFIS is a fuzzy inference system introduced in the work structure of an adaptive neuro-fuzzy network. Using a hybrid learning procedure, the ANFIS system is able to build an input-output map based on human knowledge and on input/output data pairs. The ANFIS method is superior to other modeling methods such as the autoregressive model, cascade correlation neural networks, back-propagation neural networks, sixth-order polynomials, and linear prediction methods [23].

3. Case study

3.1. In-process grinding monitoring by acoustic emission

This case aims to investigate the efficiency of digital signal processing tools of acoustic emission signals in order to detect thermal damages in grinding process. To accomplish such goal, an experimental work was carried out for 15 runs in a surface grinding machine operating with an aluminum oxide grinding wheel and ABNT 1045. A high sampling rate data acquisition system at 2.5 MHz was used to collect the raw acoustic emission. Many statistics have shown effective to detect burn, such as the RMS, correlation of the AE, CFAR, ROP and MVD. However, the CFAR, ROP, Kurtosis and correlation of the AE have been presented more sensitive than the RMS.

3.1.1. Experimental setup

The experimental tests were carried out upon a surface grinding machine where raw acoustic emission signals were collected for fifteen different runs at 2.5 million of samples per second rate. Data was collected from a fixed acoustic emission sensor of the Sensis manufacturer; model PAC U80D-87, which was mounted on the part holder. The major

grinding parameters were kept constant during the runs, and can be seen in Table (1). However, the depth of cut was varied from light and aggressive cutting. All the parts were essayed post-mortem and the burn marks were identified.

Items	Specifications and conditions
Grinding wheel	Type: 38A80-PVS-Norton, size: 296.50 x 40.21 mm
Wheel speed	27.94 m/s (1800 rpm)
Coolant	Type: water-based fluid 4%
Workpiece	Material: ABNT 1045 steel, size: 98.58 x 8.74 mm
Workpiece speed	0.044 m/s

Table 1. Experimental specifications and conditions.

The Table (2) shows details of tests carried out for the ABNT 1045 steel. Besides the visual analysis, roughness and microhardness test were performed on the parts.

Test	Depth of cut (µm)		Cutting Profile	Comments
1	10			No burn
2	30			Slight burn
3	20			Severe burn
4	90	10		Severe burn
5	20	2.5		Severe burn
6	40	5		Severe burn
7	15			Burn at middle

Table 2. Tests with ABNT 1045 steel.

3.1.2. Results

Digital processing of the acoustic emission signals was accomplished for many statistical correlations such as kurtosis, skewness, autocorrelation, RMS, CFAR, ROP and MVD. These statistics were obtained by digitally processing the raw acoustic emission in blocks of 2048 samples. As a result, each statistics were computed along the 6 second-related test, which was composed of the grinding pass itself and some noise period before and after the grinding pass. The graphs for each workpiece obtained for these statistics are presented in Figure (2) for tests 1, 5 and 7 respectively.

From the results it can be observed that the RMS statistic had a stable level for the non-burning workpiece during all over the grinding pass while significant variations can be observed when severe burn occurred, as can be seen in Figure (2a) for non-burning and Figure (2b) for severe burning. Skewness and kurtosis presented variation when burn took place but positive amplitudes dos some tests and negative ones for others were observed, which are not useful for an indicator parameter to burn. The ROP turned out to be a good indicative to burn, since its behavior has shown quite sensitive to the studied phenomenon. Besides, its level is low to those non-burning parts and high to the burning ones.

Additionally, it has well characterized the contact between the wheel and piece. The MVD tool presented a behavior similar to the RMS statistic. The autocorrelation statistic was very sensitive to burn for the most tests performed but for a few it has shown useless by virtue of the decreasing observed when burn occurred. Similarly to the autocorrelation, the CFAR tool has behaved quite well to burn detection for most of the tests carried out but with no decreasing of signal at all, except for test 7 where a decreasing was observed during the grinding pass. This behavior, however, did not compromise the utility of CFAR tool, for the level of test 7 has kept higher than to the non-burning test.
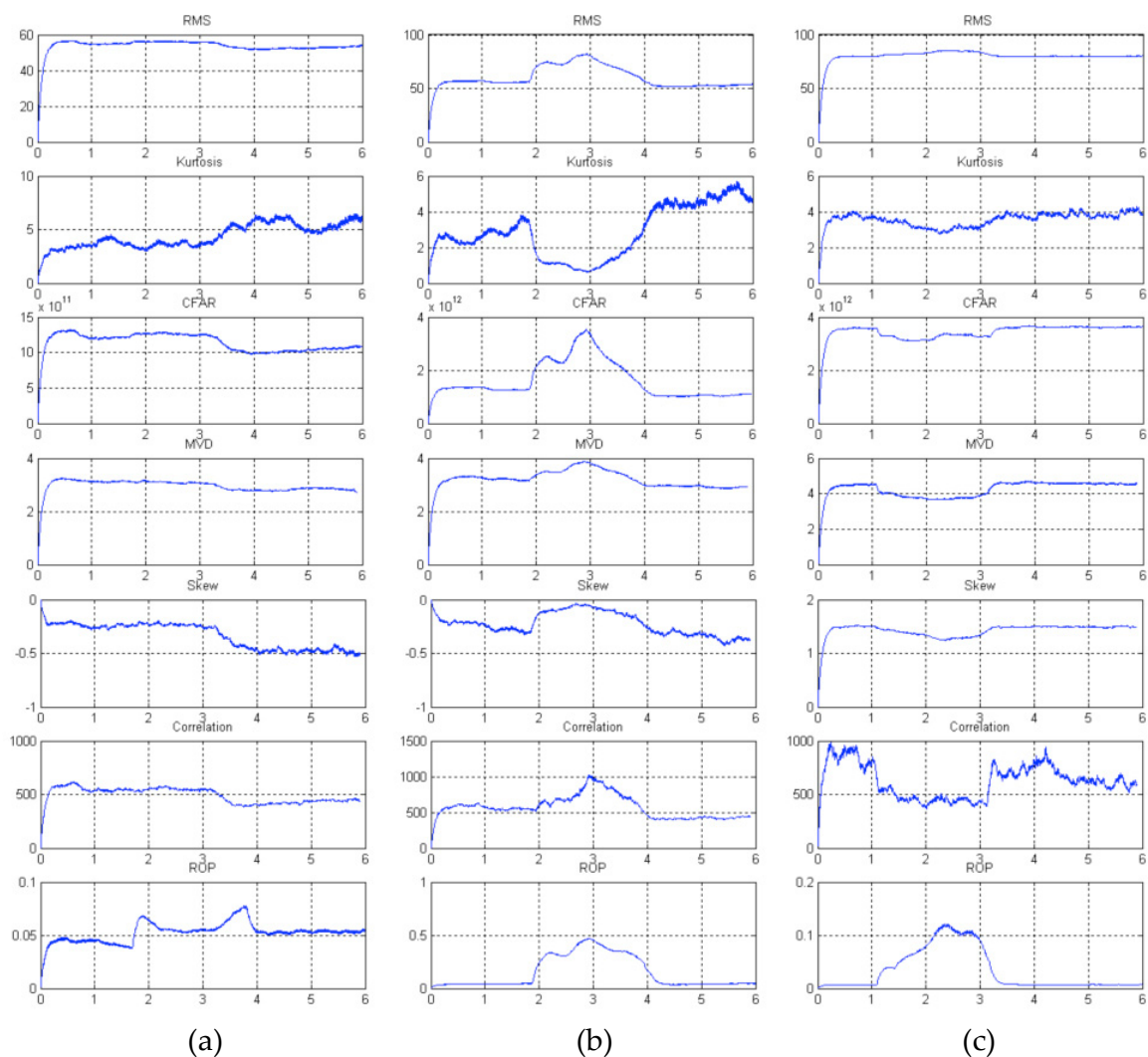

(a)   (b)   (c)

Figure 2. Results for Test 1, Test 5 and Test 7; Horizontal axis corresponds time in seconds and Vertical axis Volts multiplied by a constant; (a) Test 1 with no burn; (b) Test 5 with severe burn from close to the beginning to the end; (c) Test 7 with burn in the midst.

3.1.3. Case study conclusion

For this case study, the results show that several statistics have worked quite well to burn detection, as is the case of RMS, CFAR, ROP and MVD. Nevertheless, skewness and kurtosis statistics have presented an interesting behavior regarding the waveform of the signal and their variation along the grinding pass, though they are not effective to detect burn.

3.2. Classification of burn degrees in grinding by neural nets

The aim of this case study is to attain the classification of burn degrees of the parts ground with the utilization of neural networks. The acoustic emission and power signal as well as the statistics derived from the digital signal processing of these signals are utilized as inputs of the neural networks. The results have shown the success of classification for most of the structures studied.

3.2.1. Experimental setup

A surface grinding machine was used in the grinding tests equipped with an aluminum oxide grinding wheel, model ART-FE-38A80PVH. An acoustic emission sensor was placed near the workpiece and an electrical power transducer for measuring the electrical power consumed by three-phase induction motor that drives the wheel were employed. The acoustic emission (AE) and cutting power (Pot) signals were measured at 2.0 millions of samples per second. Table (3) list the parameters adjusted to the system.

Items	Specifications and conditions
Wheel speed	30 m/s (1800 rpm)
Coolant	Type: water-based fluid 4%
Workpiece	Material: SAE 1020 steel, size: 150 x 10 x 60 mm
Workpiece speed	0.033 m/s

Table 3. Experimental specifications and conditions.

The power transducer consists of a Hall sensor to measure the electric current and a Hall voltage sensor to measure the voltage at the electric motor terminals. Both signals are processed internally in the power transducer module by an integrated circuit, which delivers a voltage signal proportional to the electrical power consumed by the electric motor.

The tests were carried out for 12 different grinding conditions, and subsequently the burn degrees (no-burn, slight burn, medium burn, and severe burn) could be visually assessed for each workpiece surface. Dressing parameters, lubrication and peripheral wheel speed were adequately controlled in order to ensure the same grinding condition for each test. Each run consisted of a single grinding pass along the workpiece length at a given grinding condition to be analyzed.

3.2.2. Results

The digital signal processing phase started after all the 12 tests were carried out. The process generated seven new statistics, that is, the parameters DPO and DPKS, and the statistics CFAR and MVD. Seven structures were used for the neural network implementation as shown in Table (4). It can be noted in this table that besides the signals and statistics aforementioned the depth of cut a was also used as input.

In this case, the back-propagation algorithm of neural networks, which is one of the learning models, was used. The following parameters ware also found more suitable: downward gradient training algorithm; all data in the neural networks were normalized; training for 1000 epochs; square mean error value of 10-5. Cross-validation was used to estimate the generalization error of the model. The outputs of the neural network was configured in a binary way according to the degree of burn obtained, that is, 0001 for no no-burn, 0010 for slight burn, 0100 for medium burn, and 1000 for severe burn.

Structure	Inputs
I	Pot, AE, a
II	DPO, a
III	DPKS, a
IV	MVD, a
V	CFAR, a
VI	AE, a
VII	Pot, a

Table 4. Neural Network Structures.

Each statistic was represented by a vector of 3000 samples for each test subsequently the digital processing of the AE and power signals. The quantification of the grinding burn on every part surface was done by specific software for that purpose, which assessed the surface of a given part regarding the burn level through its digitalized picture. From the results of this characterization, input vectors ware separated and assigned to the corresponding type of burn. The input vectors were again divided into training, validation and test vectors.

Then, the process of optimization for the neural network was carried out. For each structure were tested some parameters like the number of neurons of the hidden layer, learning rate and momentum. The best results for all structures were obtained and presented in Table (5).

Structure	Neurons	Learning rate	Momentum
I	3 – 35 – 4	0.7	0.6
II	2 – 50 – 4	0.7	0.3
III	2 – 45 – 4	0.5	0.7
IV	2 – 30 – 4	0.3	0.7
V	2 – 50 – 4	0.7	0.3
VI	2 – 40 – 4	0.7	0.7
VII	2 – 20 – 4	0.5	0.3

Table 5. Final configuration for the 7 neural network structures.

The results for each structure were generated by inputting the corresponding data along with the depth of cut information, and the network output was interpreted in a bar graph fitting the form of the ground workpiece according to each burn level obtained. The digital picture of the workpiece with the corresponding bar graph for each structure was put all together for comparisons.

Figure (3) shows the results obtained when the signal vectors of Test 2, not used in the training, were inputted to the neural network. Thus, the data given to neural network are different from those it was used in training, testing this way its ability of classifying the burn levels. It can be observed that the structures were able to detecting well the changes in the burn levels occurred in this test. Some minor errors of classification were also observed as is the case of the Structure IV, Figure (3e), which has failed in classifying severe burn in the end of the workpiece.

Figure 3. Results obtained for Test 2; (a) Workpiece picture; (b) Structure I; (c) Structure II; (d) Structure III; (e) Structure IV; (f) Structure V; (g) Structure VI; (h) Structure VII.

It can be observed in Figure (4) that all structures have presented a success rate quite good, with the exception of Structure IV that has presented a success rate of only 52.9%. The structure having acoustic emission, power and depth of cut was supposed to own a better position in the grading since these signals are widely employed in the grinding process monitoring. On the other hand, Structure II composed by DPO parameter and depth of cut has present the best result, this can also be explained due to the parameter DPO combines the variations of the RMS acoustic emission and the maximum amplitude of the electric power during the grinding pass, resulting in an excellent tool for detection of burn degrees. It can be emphasized that all structures detected slight burn quite well, and the grading showed was based on the success rate for all degrees of burn studied.
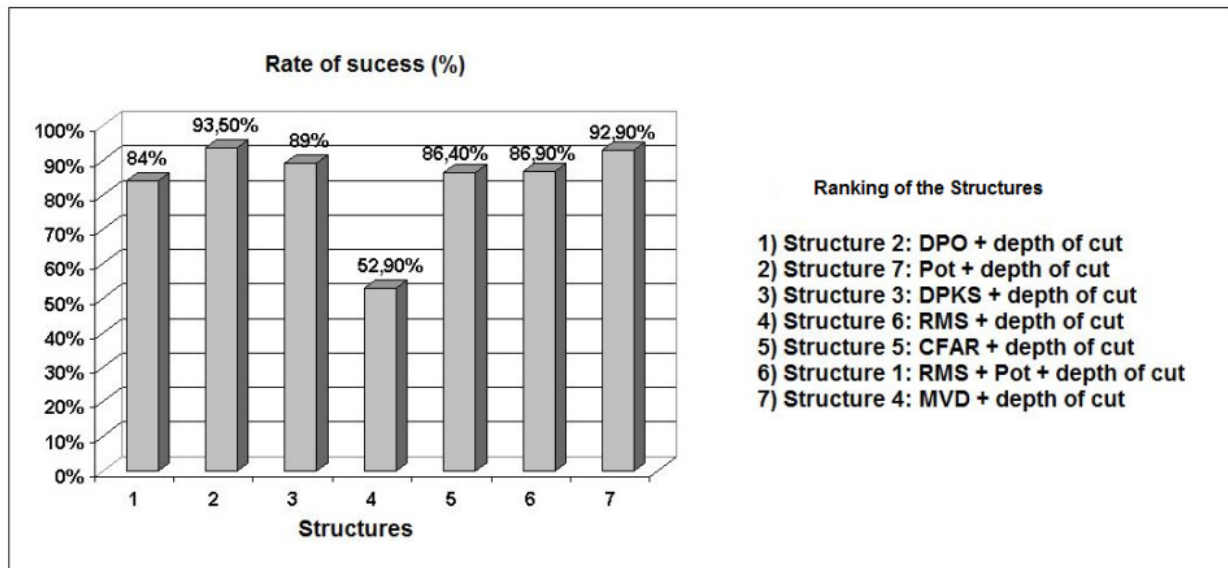
Figure 4. Rate of success for each structure and the ranking obtained.

3.2.3. Case study conclusion

The utilization of neural network of type multi-layer perceptron using back-propagation algorithm guaranteed very good results.

As all structures have detected correctly the degree of slight burn that is the first stage of change on thermal damage, it can be concluded that all structures worked well for classification of burn or non-burn occurrence.

The differences of errors found among the Structures II, VI and VII are quite small, that is, less than 1% for the set of input #7, and 6.6% for the set of input #6 with respect to Structure II. Therefore, the acoustic emission and electric power signals can also be employed successfully as inputs to the artificial neural networks for classification of burn degrees in grinding.

3.3. ANFIS applied to the prediction of surface roughness in grinding of advanced ceramics

In this case is introduced a methodology for predicting the surface roughness of advanced ceramics using Adaptive Neuro-Fuzzy Inference System (ANFIS). For this work, alumina workpieces were pressed and sintered into rectangular bars. The statistical data processed from the AE signal and the cutting power, were used as input data for ANFIS. The output values of surface roughness were implemented for training and validation of the model. The results indicated that an ANFIS network could predict the surface roughness of ceramic workpieces in the grinding process.

3.3.1. Experimental setup

To evaluate the behavior and collect the signals in surface grinding process of advanced ceramics, a test bench was created. A surface grinding machine was used, equipped with a synthetic diamond grinding wheel (type: SD 126 MN 50 B2). Dressing was carried out with a cluster type diamond dresser. The test pieces, consisted of rectangular bars of commercial alumina comprising 96% of aluminum oxide and 4% of flux oxides, were produced by pressing and sintering. Table (6) lists the parameters adjusted to the system.

A piezoelectric type sensor attached to the holder that fixes the workpiece collected the AE signal. The system's cutting power was recorded through an electrical power module connected to the power supply of the frequency converter. Surface roughness was measured with a Taylor Hobson Surtronic 3+ surface roughness tester. Tests were performed at three different cutting depths: 20μm, 70μm and 120μm to record the signals and surface roughness data.

The following statistics was obtained from the cutting power and AE signals: mean of AE, standard deviation of AE (std of AE), mean of cutting power (mean of PW), standard deviation of cutting power (std of PW), DPO and DPKS. These values were evaluated as inputs to the ANFIS system. Based on the surface roughness values, regressions were made to obtain more data for training the networks. Figure (5) illustrates this process.

Items	Specifications and conditions
Wheel speed	35 m/s (1800 rpm)
Workpiece speed	0.038 m/s
Coolant	Type: Conventional water and oil emulsion (Rocol Ultracut 370); Concentration: 5%
Fluid velocity	3 m/s
Fluid outflow	27.5 l/min (0.458 l/s)
Pressure of the fluid in the system	Lower than 0.2 kgf/cm2

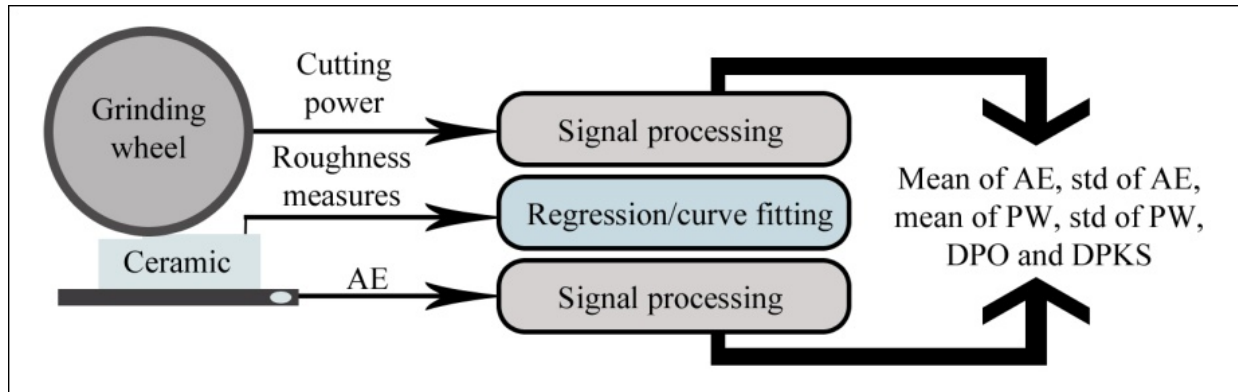**Table 6.** Experimental specifications and conditions.

Figure 5. Data acquisition and signal processing scheme.

3.3.2. Results

For this case, the ANFIS model with three inputs composed by: acoustic emission, standard deviation of power and the DPO statistic. This model presented the lowest error and best represent the behavior of the system.

For the best model was conduced several test to find the ideal training parameters. The number of membership functions per input was varied, and the general error of the test set and the general error related to the real measurements were analyzed.

Table (7) lists the final parameters of the definitive ANFIS model for the prediction of surface roughness of a ceramic body. The five rules are in the form: Rule(k) – IF (mEA is In1cluster(k)) and (sPot is In2cluster(k)) and (DPO is In3cluster(k)) THEN (Roughness Outcluster(k)), where k is the rule number and varies from 1 to 5.

Parameter	Value
Number de Membership Functions per Input	5
Type of Membership Function	Gbellmf, Gaussian function
Target Error	0.001
Maximum Number of Iterations	100
Maximum Learning Coefficient	1.1
Training Method	Hybrid

Table 7. Definitive parameters of the ANFIS model.

The newly created model was validated using values generated by the surface roughness curve. The result is depicted in Figure (6), which shows a good prediction with a total error of approximately 4%.
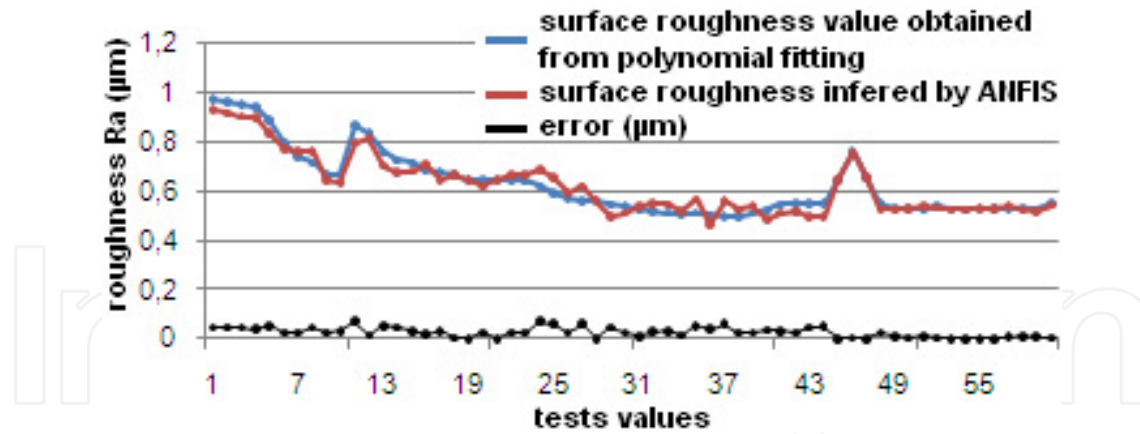
Figure 6. Inference of surface roughness by ANFIS for the test set generated by the fitted roughness curve.

3.3.3. Case study conclusion

The accuracy of the ANFIS network for predicting surface roughness demonstrates that this type of network is a good data prediction system, since its hybrid nature (neural and fuzzy) enables the correct prediction of the values of the system, which are not easily related.

The ANFIS network tested with three inputs showed a lower RMS error than the networks with one and two inputs, and the best set was the one whose parameters were the mean acoustic emission, the standard deviation of cutting power and the DPO.

The predicted surface roughness values showed a percent error of 7.54% for the measurements taken in the tests at 20μm of depth, 6.54% for the test at 120μm, and the lowest error of 4.73% for the test at 70μm. After building the ANFIS model and training it, it was possible to obtain the membership functions, with their allocated centers, the rule sets for predicting surface roughness, and the set of output equations of the model, enabling the system's application in a control environment.

4. Conclusions

The characterization and detection of anomalies during the grinding process were successfully performed by digitally processing the raw acoustic emission signal for several statistics studied and presented in this chapter. The first case study has shown good results for burn detection with the statistics RMS, CFAR, ROP and MVD.

Artificial neural networks (ANNs) proved to be very useful tool for pattern recognition of grinding burn degrees as well as estimating the wear of the grinding wheel indirectly. In addition, ANNs have presented good results in estimating surface roughness of advanced ceramics. This turns out to be a benefit towards the optimization of the grinding process, avoiding high reject rates, scrap, rework, and machine downtime.

Based on the studies presented, a contribution is given to the development of a database needed to determine the control parameters of the grinding process. It is therefore possible

to determine safe regions to operate the grinding machine from mild to critical conditions, providing a system to the end user to start out with the optimal parameters, eliminating the need for trial and error, with increased productivity, reduced expenditures on consumables, scrap and rework reduction, and improved quality. The digital signal processing of the raw acoustic emission as well as the artificial neural network models applied to the grinding process provide valuable information necessary to optimize the process.

Author details

Paulo R. Aguiar, Cesar H.R. Martins, Marcelo Marchi and Eduardo C. Bianchi
Universidade Estadual Paulista "Júlio de Mesquita Filho" (UNESP), Bauru campus, Brazil

5. References

[1] Pham, D. T. & Pham, P. T. N. (1999). Artificial intelligence in engineering. *International Journal of Machine Tools & Manufacture*, Vol.39, No.6, pp. 937-949, ISSN 0890-6955

[2] Aguiar, P. R.; Willet, P. & Webster, J. (1999). Acoustic emission applied to detect workpiece burn during grinding, In: *Acoustic emission: Standards and Technology Update, ASTM STP 1353*, S. J. Vahaviolos, (Ed.), 107-124, American Society for Testing and Materials, ISBN: 0-8031-2498-8, West Conshohocken, Pennsylvania, USA.

[3] Aguiar, P. R.; Cruz, C. E. D.; Paula, W. C. F.; Bianchi, E. C.; Thomazella, R.; Dotto, F. R. L. (2007). Neural network approach for surface roughness prediction in surface grinding, *Proceedings of the 25th IASTED International Multi-Conference: Artificial Intelligence and Applications*, Innsbruck, 2007, pp. 96-106.

[4] Aguiar, P. R.; Souza, A. G. O.; Bianchi, E. C.; Leite, R. R.; Dotto, F. R. L. (2009). Monitoring the Dressing Operation in the Grinding Process, *International Journal of Machining and Machinability of Materials*, 5 (1), pp. 3-22.

[5] Inasaki, I. (1999). Sensor fusion for monitoring and controlling grinding processes, *The International Journal of Advanced Manufacturing Technology*, Vol.15, No.10, pp. 730-736, ISSN 0268-3768.

[6] Bennett, R. T (1994). *Acoustic emission in grinding*, Master Thesis, University of Connecticut.

[7] Webster, J.; Marinescu, I.; Bennett, R. & Lindsay, R. (1994). Acoustic emission for process control and monitoring of surface integrity during grinding, *CIRP Annals – Manufacturing Technology*, Vol.43, No.1, pp. 299-304, ISSN 0007-8506.

[8] Sachse, W.; Roget J.; Yamaguchi, K. (1991). Acoustic Emission: Current Practice and Future Directions, ASTM.

[9] Dornfeld, D. A. (1990). Neural network sensor fusion for tool condition monitoring, *Annals of the CIRP*, Vol.39, No.1, pp. 101-105.

[10] Fang, X. D. (1995). Expert system-supported fuzzy diagnosis of finish-turning process states, *International Journal of Machine Tools Manufacturing*, Vol.35, No.6, pp. 913-924, Elsevier Science.

[11] Nuttal, A (1997). Performance of power-law processors with normalization for random signals of unknown structure, Naval Undersea Warfare Center, *NPT Technical Report 10,760.*

[12] Nuttal, A. (1996). Detection performance of power-law processors for random signals of unknown location, structure, extent, and strength, *AIP Conference Proceedings*, Vol.375, No.1, pp. 302-324, ISBN 1-56396-443-0.

[13] Wang, Z. (1999). Surface grinding monitoring by signal processing of acoustic emission signals, Master Thesis, University of Connecticut.

[14] Chen, B.; Willett, P.; Streit, R. (1999) Transient detection using a homogeneity test, in: Proceedings of 1999 ICASSP, Phoenix, AZ, no. 1715, IEEE, Piscataway, New Jersey.

[15] Wang, Z.; Willet, P.; Aguiar, P. R. & Webster, J. (2001). Neural network detection of grinding burn from acoustic emission, *International Journal of Machine Tools & Manufacture*, Vol.41, No.2, pp.283-309, ISSN 0890-6955.

[16] Oppenheim, A. V. et al. (1997). Signals & Systems, 2sd. Edition, Prentice Hall Signal Processing Series.

[17] Aguiar, P. R.; Bianchi, E. C.; Oliveira, J. F. G. A. (2002). Method for Burning Detection in Grinding Process Using Acoustic Emission and Effective Electrical Power Signals. In: CIRP Journal of Manufacturing Systems. Paris, v.31, n.3, 253 – 257.

[18] Dotto, F. R. L.; Aguiar, P. R.; Bianchi, E. C.; Serni, P. J. A. & Thomazella, R. (2006). Automatic system for thermal damage detection in manufacturing process with internet monitoring. *Journal of Brazilian Society of Mechanical Science & Engineering*, Vol.28, No.2, pp. 153-160, ISSN 1678-5878.

[19] Kwak, J. S. & Song, J. B. (2001). Trouble diagnosis of the grinding process by using acoustic emission signals, *International Journal of Machine Tools & Manufacture 41*, pp. 899-913.

[20] Nathan, R. D.; Vijayaraghavan L.; Krishnamurthy R. (1999). In-process monitoring of grinding burn in the cylindrical grinding of steel, Journal of Materials Processing Technology, 91, 37–42.

[21] Musavi, M.; Ahmed, W.; Chan, K.; Faris, K. (1992). On the Training of Radial Basis Function Classifiers, Neural Networks, 5, pp. 595-603.

[22] Hopgood, A. A. (2000). Intelligent Systems for Engineers and Scientists, 2nd. Edition, Boca Raton: CRC Press.

[23] Jang, J. S. R. (1993). ANFIS: Adaptive-network-based fuzzy inference system, IEEE Transactions on Systems, Man and Cybernetics, 23 (3), 665-685.

[24] Sugeno, M. & Kang, G. T. (1988). Structure identification of fuzzy model, Fuzzy Sets and Systems, 28, 15-33.

[25] Takagi, T. & Sugeno M. (1985). Fuzzy identification of systems and its aplications to modeling and control, IEEE Trans. Syst Man Cyber, 15, 116-131.

[26] Lezanski, P. (2001). An intelligent system for grinding wheel condition monitoring, Journal of Materials Processing Technology, 109, 258-263.

[27] Chiu, S. L. (1994). Fuzzy model identification based on cluster estimation, Journal of Intelligent and Fuzzy Systems, 2, 267-278.

[28] Chiu, S. L. (1996). Selecting input variables for fuzzy models, Journal of Intelligent and Fuzzy Systems, 2, 267-278.

[29] Lee, K. C.; Ho, S. J.; Ho, S. Y. (2005). Accurate estimation of surface roughness from texture features of the surface image using an adaptive neuro-fuzzy inference system, Precision Engineering, 29, 95-100.